# Accepted Manuscript


Hyperbranched polymers with aggregation-induced emission property for solution-processed white organic light-emitting diodes

Dongyu Wu, Tiaomei Zhang, Jing Sun, Yuling Wu, Xiaoqing Liao, Guojing Lu, Jingjing Yang, Hua Wang, Lu Li, Bingshe Xu

PII: S0040-4020(18)31280-8

DOI: https://doi.org/10.1016/j.tet.2018.10.057

Reference: TET 29890

To appear in: *Tetrahedron*

Received Date: 14 August 2018

Revised Date: 1 October 2018

Accepted Date: 23 October 2018

Please cite this article as: Wu D, Zhang T, Sun J, Wu Y, Liao X, Lu G, Yang J, Wang H, Li L, Xu B, Hyperbranched polymers with aggregation-induced emission property for solution-processed white organic light-emitting diodes, *Tetrahedron* (2018), doi: https://doi.org/10.1016/j.tet.2018.10.057.

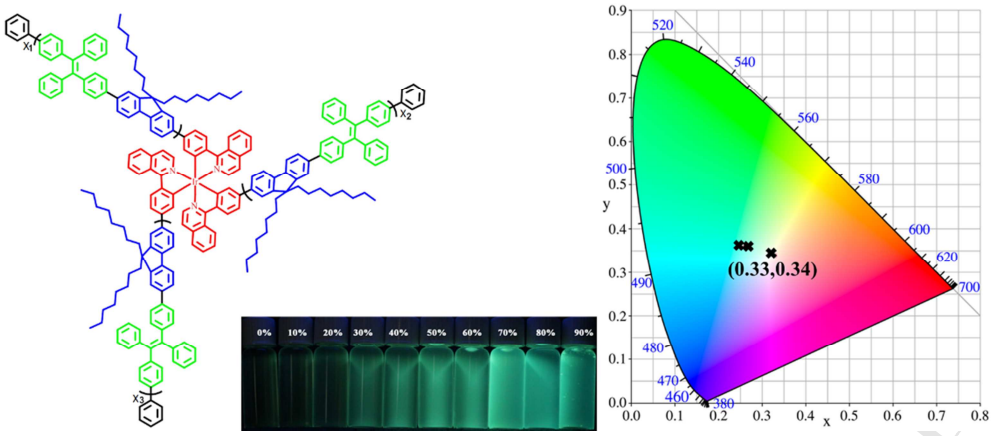


A series of hyperbranched copolymers were designed and synthesized, achieving the aggregation-induced emission (AIE) and a Commission International de l'Eclairage coordinate of (0.33, 0.34).

# Hyperbranched polymers with aggregation-induced emission property for solution-processed white organic light-emitting diodes

Dongyu Wu[a, b], Tiaomei Zhang[a, b], Jing Sun[a, b], Yuling Wu[a, b], Xiaoqing Liao[c], Guojing Lu[a, b], Jingjing Yang[a, b], Hua Wang[a, b, *], Lu Li[c, **], Bingshe Xu[a, b]

[a] Key Laboratory of Interface Science and Engineering in Advanced Materials, Ministry of Education, Taiyuan University of Technology, Taiyuan 030024, PR China

[b] Research Center of Advanced Materials Science and Technology, Taiyuan University of Technology, Taiyuan 030024, PR China

[c] Co-innovation Center for Micro/Nano Optoelectronic Materials and Devices, Research Institute for New Materials and Technology, Chongqing University of Arts and Sciences, Chongqing 402160, PR China

## ABSTRACT

In this work, a new series of hyperbranched polymers of PFTPE-Ir(piq)$_3$-X(X=1, 5, 10) were designed and synthesized, in which tris(1-phenylisoquinoline)iridium(Ⅲ) (Ir(piq)$_3$) acts as red emission core and PFTPE acts as branches. The photophysical study reveals that these hyperbranched polymers exhibit aggregation-induced emission (AIE) characteristic, inducing in much higher photoluminescent quantum yield ($\Phi_Y$) in neat film than that in dilute tetrahydrofuran (THF) solution. The white-light OLEDs using PFTPE-Ir(piq)$_3$-X as emission layer show rather weaker efficiency roll-off. Especially, the white-light OLED based on

PFTPE-Ir(piq)$_3$-5 as emission layer shows a maximum luminance of 4686 cd/m$^2$, a maximum luminous efficiency of 2.43 cd/A, a maximum external quantum efficiency of 1.08% and the Commission Internationale de l'Eclairage coordinate of (0.26, 0.36).

**KEYWORDS:** white-light; OLED; aggregation-induced emission; hyperbranched polymers

## 1. Introduction

Different from illumination source of light emitting diodes (LED), white-light organic light emitting devices (WOLEDs) owing to such properties as high contrast, lightweight, and flexibility have gained plenty of attention recently. In addition, WOLEDs provide a novel approach to achieve large-area solid state lighting by wet-processes, which are regarded as potential candidates for next-generation illumination sources in the future [1-5]. In the last decades, WOLEDs with various kinds of device architectures have been fabricated [6-11], such as multilayer architectures with different emitting polymers, multilayer phosphorescent emitters and single layer with doping systems of polymers [12-15]. However, owing to intrinsic phase separation, WOLEDs with above architectures show rather lower luminous yield and shorter lifetime. Thus, it is very important and practical to design and synthesize white-light polymers composed of different color light-emitting units by conjugation of covalent bonding, which can act as single emission layer to impel reduction of heterogeneous interfaces and improve device performance of WOLEDs [16-19]. At present, the triple-color white-lightpolymers have been reported and attracted widespread attention [20,21]. Conjugated copolymers derived from polyfluorene with phosphorescent emitter have been demonstrated to achieve efficient white light emission. Phosphorescent light emitting units are

introduced in linear structures of poly(9,9-dioctylfluorene) (PFO), which serve as single emission layer to improve device performance of WOLEDs [20,21]. For instance, the triple-color white-light polymers have been prepared and reported by Prof. Cao's group, in which bis(1-phenylisoquinoline)(dibenzoylmethane)iridium(III) and fluorenone groups are introduced into PFO chains as red light units and green light units, respectively [22]. Nevertheless, conjugation interactions between adjacent chains in linear polymers might lead to lower luminous efficiency and worse stability of WOLED.

It had been known that hyperbranched polymers with three-dimensional structure exhibit larger space steric hindrance, which can markedly restrain intermolecular interactions and aggregation between the adjacent polymers [23-25]. Moreover, they also possess such properties as good solubility, minimization of unfavorable crystallization and excellent film-forming property, which can satisfy the demands of fabrication WOLEDs by ink-jet printing.

As mentioned above, property of white-light polymer can be improved by introducing hyperbranched structure, especially, the separation of surrounding long conjugation chains can improve efficiency stability in some extent. But, the long conjugation chains twine around each other in film state, which induces in fluorescence aggregation-caused quenching (ACQ) effect. Hence, WOLEDs based on hyperbranched polymers show some efficiency roll-off phenomenon in high current density. Fortunately, fluorescence aggregation-induced emission (AIE) as a remarkable phenomenon was first reported by Prof. Tang's group since 2001, which has developed explosively and gained remarkable attention in these years [26]. To explain the unconventional AIE phenomenon, the restriction of intramolecular rotation is

demonstrated as the mechanism based on valid evidence [27,28]. Compared with traditional organic luminophores, AIE luminogens (AIEgens) enjoy many advantages in aggregated state, for example, high brightness, high luminous efficiency and excellent photostability, which have been utilized in OLEDs [29-32]. Among reported AIEgens, tetraphenylethene (TPE) with twisted configurations is the most representative one. In dilute tetrahydrofuran (THF) solution, TPE is practically nonluminescent, while, the fluorescence is dramatically enhanced with adding poor solvent water into THF, attributing to the principle of restricted intramolecular rotation (RIR) to weak π-π stacking interactions in solid state [33]. Based on above points, insertion of AIEgens of TPE in hyperbranched polymer is expected to restrain ACQ conjugation chains and improve efficiency stability eventually.

Here, a series of white-light hyperbranched polymers were designed and synthesized, in which tris(1-phenylisoquinoline)iridium(III)($Ir(piq)_3$) serves as red phosphorescent cores and PFO inserting AIEgen of TPE acts as branches. By adjusting content of red phosphorescent core of $Ir(piq)_3$, a series of white-light hyperbranched polymers were synthesized, which were also used as single emission layer of WOLEDs. They expressed nearly no efficiency roll-off under high current density [34-36].

## 2. Experimental section

### *2.1 Materials*

All commercially available reagents were not further purified unless otherwise specified. The solvents (e.g. dichloromethane, tetrahydrofuran, methanol and chloroform) were purified by conventional procedures. The synthetic routes can be seen in Scheme 1. During synthesizing process, the 1,2-Bis(4-bromophenyl)-1,2-diphenylethene (**$M_1$**) [37,38] and

tris(1-(4-bromophenyl)isoquinoline)iridium(Ⅲ)($Ir(piqBr)_3$) (**$M_2$**) were prepared according to references [23,25]. The **$M_3$** was purchased from J&K Scientific Company directly.

*2.2 Synthetic Section*

*1) 1,2-Bis(4-bromophenyl)-1,2-diphenylethene (**$M_1$**)*

The 4-bromobenzophenone (1.50 g, 5.77 mmol) dissolved in THF with addition of zinc dust (2.00 g, 30.77 mmol), which was cooled down to 0 $^{o}$C. After being stirred for 30 minutes under nitrogen protection, the $TiCl_4$ (1.72 g, 9.09 mmol) was dropped into the mixture. Then, the reaction solution refluxed overnight, which was chilled down to room temperature and concentrated. The concentrated solution was poured into 1 M HCl solution, and then extracted three times by DCM. The organic phase was dried with $MgSO_4$. The crude product was purified by silica gel column chromatography after filtration and solvent evaporation, the organic solvents petroleum ether and dichloromethane as eluent. A white solid of **$M_1$** was obtained in 70.7% yield (1.06 g). $^{1}$H NMR (600 MHz, $(CD_3)_2OS$)：δ (ppm) 7.27 – 7.21 (m, 4H), 7.16 – 7.12 (m, 3H), 7.12 – 7.09 (m, 3H), 7.00 (ddd, J = 9.8, 6.6, 3.1 Hz, 4H), 6.88 (dt, J = 10.9, 5.4 Hz, 4H). $^{13}$C NMR (151 MHz, $(CD_3)_2OS$)：δ (ppm) 145.79 (d, J = 14.3 Hz), 145.25 (d, J = 13.8 Hz), 143.23 (s), 135.78 (d, J = 3.2 Hz), 134.21 – 133.95 (m), 133.81 (s), 130.93 (s), 130.73 (s), 129.80 (d, J = 17.1 Hz), 123.71 (s), 123.58 (s). Element anal. calcd (%): C, 63.70; H, 3.70. Found (%): C, 64.18; H, 3.76.

*2) tri(1-(4-bromophenyl)isoquinoline)iridium(III) ($Ir(piqBr)_3$) (**$M_2$**)*

The 1-chloroisoquinoline (2.45 g, 15 mmol), 4-bromophenylboronic acid (3.00 g, 15 mmol) and $Pd(PPh_3)_4$ were dissolved in the mixed solution of degassed toluene, ethanol and $Na_2CO_3$ aqueous solution. Then, the resulting mixture was slowly heated to 90℃. Finally, the

1-(4-bromophenyl)-isoquinoline was purified by column chromatography. Tri(acetylacetonato)iridium(III) (488 mg, 1 mmol) and 1-(4-bromophenyl)-isoquinoline (994 mg, 3.5 mmol) were added into anhydrous glycerol. The reaction solution was slowly heated to 220□. Finally, the product of tri(2-(4-bromophenyl)-isoquinoline)iridium(III) ($Ir(piqBr)_3$) was purified by column chromatography. $^1$H NMR: (600 MHz, $CDCl_3$): d (ppm) = 8.87 (dd, J1 = 7.2 Hz, J2 = 3 Hz, 3H), 8.03 (d, J = 8.4 Hz, 3H), 7.76 (dd, J1 = 5.4 Hz, J2 = 3 Hz, 3H), 7.70–7.67 (m, 6H), 7.29 (d, J = 6.6 Hz, 2H), 7.15 (d, J = 6.6 Hz, 3H), 7.13 (dd, J1 = 8.4Hz, J2 = 2.4Hz, 3H), 7.03 (d, J = 1.8 Hz, 3H). $^{13}$C NMR: (600 MHz, CDCl3): d (ppm) = 166.9, 165.6, 144.2, 139.7, 139.3, 136.9, 131.5, 131.0, 130.7, 129.0, 128.1, 127.5, 127.3, 123.4, 120.1.

*3) hyperbranched polymers of PFTPE-Ir(piq)$_3$-X*

Under nitrogen protection, the compounds of $\mathbf{M_1}$, $\mathbf{M_2}$ and $\mathbf{M_3}$ dissolved in toluene and stirred for 30 minutes under room temperature, in which methyl trioctyl ammonium chloride (Aliquant 336), aqueous solution of 2 M $K_2CO_3$ and $Pd(PPh_3)_4$ were added in proper order. Then, the reaction mixture was being stirred and refluxed. After 48 h, the polymers were capped by adding benzeneboronic acid and bromobenzene with continuous reaction. When the reaction was completed, the solution was cooled to room temperature and injected into large amounts of methanol. Finally, the final product was purified preliminarily and the crude product was obtained. The crude product was purified with acetone in Soxhlet extraction, which can achieve the purpose of pure solid powder.

*PFTPE-Ir(piq)$_3$-1*

The compounds of $\mathbf{M_1}$ (492.49 mg, 0.9985 mmol), $\mathbf{M_2}$ (1.04 mg, 0.001 mmol), and $\mathbf{M_3}$ (642.57 mg, 1 mmol) were used for polymerization as light yellow powder with a yield of

38.06% (310.2 mg). $^1$H NMR: (600 MHz, $CDCl_3$): δ (ppm) 7.75-7.65 (2H, Ar-H), 7.58-7.42 (4H, Ar-H), 7.23-7.06 (6H, Ar-H), 2.09-1.89 (2H, $CH_2$), 1.30-0.98 (10H, 5 $CH_2$), 0.81-0.61 (5H, $CH_2$, $CH_3$). Element anal. Calcd (%): C, 91.33; H, 8.64. Found (%): C, 91.41; H, 8.31.

*PFTPE-Ir(piq)$_3$-5*

The compounds of **$M_1$** (489.53 mg, 0.9925 mmol), **$M_2$** (5.21 mg, 0.005 mmol), and **$M_3$** (642.57 mg, 1 mmol) were used for polymerization as light yellow powder with a yield of 49.01% (400.5 mg). $^1$H NMR: (600 MHz, $CDCl_3$): δ (ppm) 7.79-7.63 (2H, Ar-H), 7.60-7.40 (4H, Ar-H), 7.22-7.02 (6H, Ar-H), 2.07-1.91 (2H, $CH_2$), 1.30-0.99 (10H, 5 $CH_2$), 0.82-0.60 (5H, $CH_2$, $CH_3$). Element anal. Calcd (%): C, 91.21; H, 8.63. Found (%): C, 88.15; H, 7.94.

*PFTPE-Ir(piq)$_3$-10*

The compounds of **$M_1$** (485.83 mg, 0.985 mmol), **$M_2$** (10.41 mg, 0.01 mmol), and **$M_3$** (642.57 mg, 1 mmol) were used for polymerization as light pink powder with a yield of 46.57% (381.3 mg). $^1$H NMR: (600 MHz, $CDCl_3$): δ (ppm) 7.77-7.63 (2H, Ar-H), 7.58-7.40 (4H, Ar-H), 7.22-7.06 (6H, Ar-H), 2.07-1.91 (2H, $CH_2$), 1.19-0.98 (10H, 5 $CH_2$), 0.81-0.62 (5H, $CH_2$, $CH_3$). Element anal. Calcd (%): C, 91.07; H, 8.61. Found (%): C, 90.32; H, 7.94.

*2.3 Instruments and characterization*

The $^1$H NMR and $^{13}$C NMR spectra were measured on a Bruker DXR 600 MHz spectrometer where the tetramethylsilane was used as internal reference for chloroform deuteride. The molecular weights of the PFTPE-Ir(piq)$_3$-X were determined by Viscotek GPC VE 3580 RI detector using THF as eluent. Thermal gravimetric analysis (TGA) curves were recorded on a Netzsch TG 209 F3 with heating rate of 10 $^o$C/min under nitrogen flow. Differential scanning calorimetry (DSC) curves were measured on TA Q2000 with heating

rate of 10 $^{o}$C/min under nitrogen flow. The cyclic voltammetry (CV) curves were measured on the Autolab/PG STAT302 electrochemical workstation with a three-electrode cell in acetonitrile (0.1 mol/L) solution of tetrabutylammonium perchlorate as electrolyte with scan rate of 50 mV/s under nitrogen atmosphere. Films of PFTPE-Ir(piq)$_3$-X were coated onto the working electrode of Pt plate and calomel electrode acted as reference electrode at room temperature. The ultraviolet-visible (UV-vis) absorption spectra and photoluminescence (PL) spectra of PFTPE-Ir(piq)$_3$-X were recorded on Hitachi U-3900 spectrophotometer and Fluoromax-4 spectrophotometer, respectively.

*2.4 Device fabrication*

The WOLEDs with configurations of ITO / PEDOT: PSS (40 nm) / PFTPE- Ir(piq)$_3$-X (80 nm) / TPBi (40 nm) / LiF (1 nm) / Al (100 nm) (Fig. 6) were fabricated by vacuum evaporation instruments equipped with glove-box. The PEDOT:PSS layer was spin-coated onto cleaned ITO glass substrates with the rotating speed of 4000 rpm, which was annealed under 120 $^{o}$C. Then, the PFTPE-Ir(piq)$_3$-X films as emission layer were spin-coated onto the PEDOT:PSS layer, which was annealed under 100 $^{o}$C. Then, the 1,3,5-tris (1-phenyl-1H-benzimidazol-2-yl)benzene (TPBi) as electron transporting layer, LiF layer and Al layer as cathode were deposited by vacuum evaporation instruments under pressures below $1\times10^{-5}$ Pa. The current density (J)-voltage (V)-luminance (L) characteristics of WOLEDs were tested on Keithley 2400 source meter and BM-7A spot brightness meter. Electroluminescence (EL) spectra were recorded through PR-655 Spectra Scan spectrometer with computer controlled. All measurements were taken at room temperature.

## 3. Results and discussion

*3.1 Synthesis and characterization*

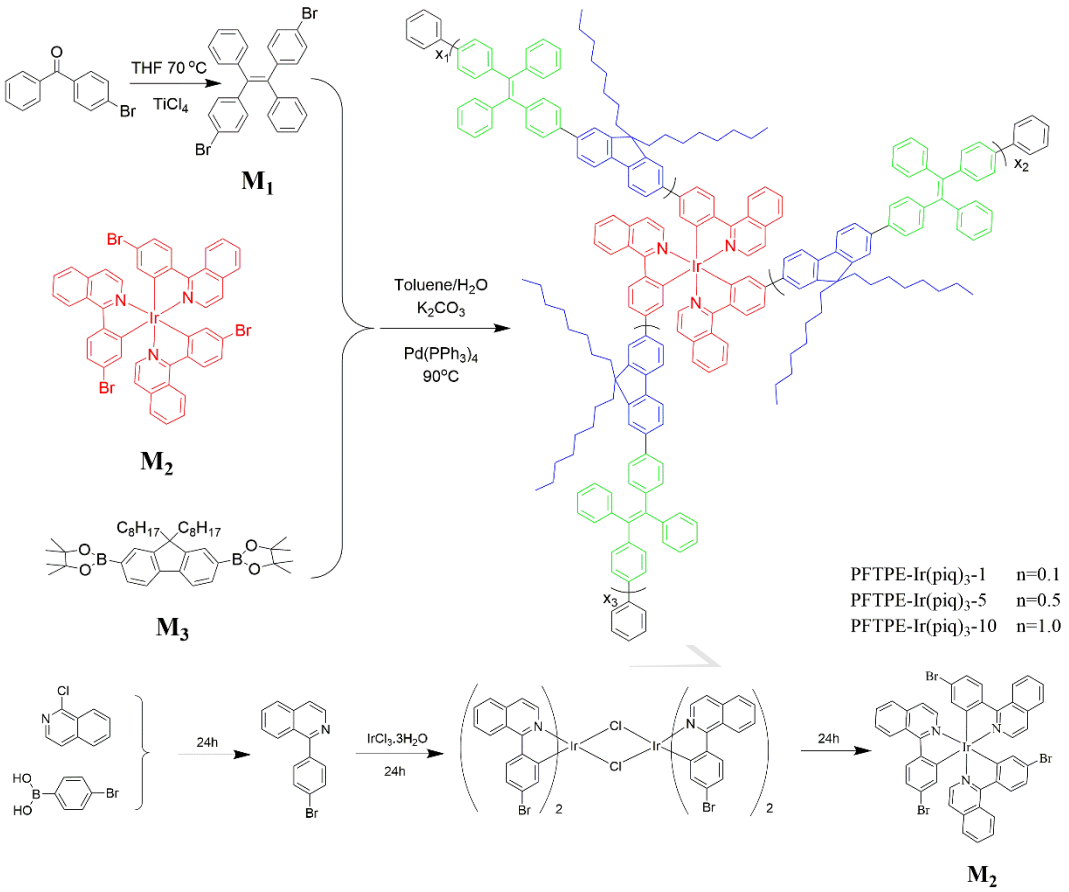


**Scheme 1.** Synthetic route of hyperbranched polymers PFTPE- Ir(piq)$_3$-X, $M_1$ and $M_2$.

The synthetic routes and chemical molecular structure of **$M_1$**, **$M_2$**, **$M_3$** and hyperbranched polymers PFTPE-Ir(piq)$_3$-X are outlined in Scheme 1. The white-light hyperbranched polymers are mainly composed of red-light phosphorescence cores of Ir(piq)$_3$ and blue-greenish fluorescence branched chains of PFTPE, which can achieve white-light emission. In the hyperbranched polymers, the Ir(piq)$_3$ are separated each other by surrounding branched chains of PFTPE, which can avoid triplet excitons annealing of Ir(piq)$_3$ owing to concentration quenching. More important, the TPE as typical AIEgen with high fluorescence quantum efficiency is inserted into branched chains, which can further improve efficiency stability of white-light hyperbranched polymer [33].

These series of PFTPE-Ir(piq)$_3$-X were synthesized by classical Suzuki coupling reaction. Firstly, Intermediates **M$_3$**, **M$_1$** and **M$_2$** were dissolved in organic solvent, respectively, which the ratios of the monomers were 1000:998.5:1, 1000:992.5:5 and 1000:985.0:10. In addition, all white-light hyperbranched polymers exhibit better thermal stability and good solubility, which can dissolve in various organic solvents. The WOLEDs based on PFTPE-Ir(piq)$_3$-X as emission layer would be fabricated by wetting-process such as spin coating or ink-jet printing [39].

The number-average molecular weights ($M_n$) and weight-average molecular weights ($M_w$) of PFTPE-Ir(piq)$_3$-X were obtained by gel permeation chromatography (GPC). The $M_w$ of PFTPE-Ir(piq)$_3$-X ranges from $13.60\times10^3$ to $19.61\times10^3$, severally, with polydispersity indices (PDIs) from 2.08 to 2.72 (Table 1). In addition, all polymers designed and synthesized have higher yield (38.06% - 49.01%).

**Table 1** Molecular weights and thermal properties of PFTPE-Ir(piq)$_3$-X.

| Polymers | Feed ratio (mol %) Ir(piq)$_3$ | $M_n$ ($\times10^3$) | $M_w$ ($\times10^3$) | PDI | $T_d$ ($^o$C) | $T_g$ ($^o$C) |
|---|---|---|---|---|---|---|
| PFTPE-Ir(piq)$_3$-1 | 0.1 | 7.22 | 19.61 | 2.72 | 404 | 134 |
| PFTPE-Ir(piq)$_3$-5 | 0.5 | 8.69 | 18.12 | 2.08 | 410 | 129 |
| PFTPE-Ir(piq)$_3$-10 | 1 | 6.37 | 13.60 | 2.14 | 405 | 131 |

*3.2 Thermal properties*

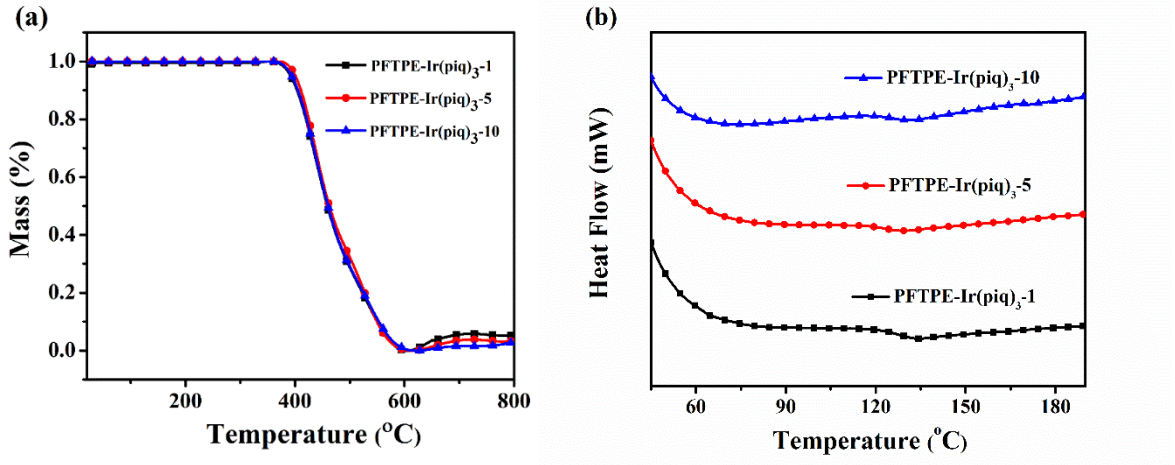


**Fig. 1.** The TGA curves (a) and DSC curves (b) of PFTPE-Ir(piq)$_3$-X.

The thermal properties of PFTPE-Ir(piq)$_3$-X were investigated as expressed in Fig. 1. The DSC curves indicate that all hyperbranched polymers of PFTPE-Ir(piq)$_3$-X exhibit higher glass transition temperature ($T_g$ = 129~134 □) in experimental temperature range (Fig. 1b). Their decomposition temperatures ($T_d$) are between 400 °C and 410 °C (corresponding to 5% weight loss), which are all higher than those of linear polymers (Fig. 1a) [40,41]. It had been identified that the hyperbranched structure can tremendously enhance thermal stability owing to stronger molecular rigidity than that of linear polymers in our early work [23-25], which would improve device lifetime.

*3.3 Optical properties*

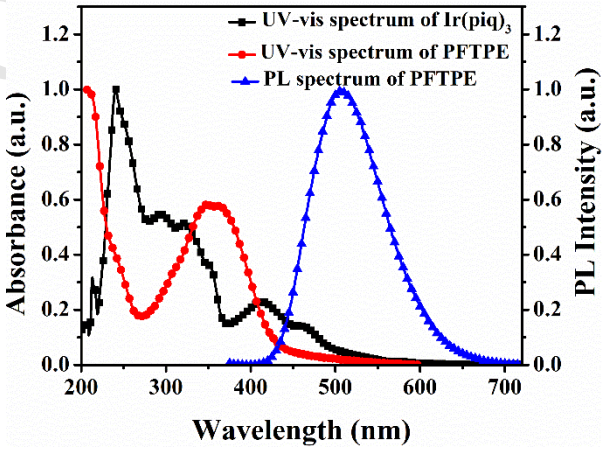


**Fig. 2.** The UV-vis absorption spectra and the PL spectra of Ir(piq)$_3$ and PFTPE in diluted

$CHCl_3$ solution ($10^{-6}$ M)

In order to discuss the luminous mechanism of PFTPE-Ir(piq)$_3$-X, the photophysical properties of Ir(piq)$_3$ and PFTPE were tested. There exist spectral overlap in the range of 420–550 nm between the UV-vis absorption spectrum of Ir(piq)$_3$ and the PL spectrum of PFTPE in Fig. 2. It manifests that Förster resonance energy transfer (FRET) from PFTPE segments to Ir(piq)$_3$ cores exists possibility, which lead to red light emission of Ir(piq)$_3$ combining with blue-greenish light emission of PFTPE. As results, through adjusting the content of Ir(piq)$_3$, white-light emission can be achieved [25,42].

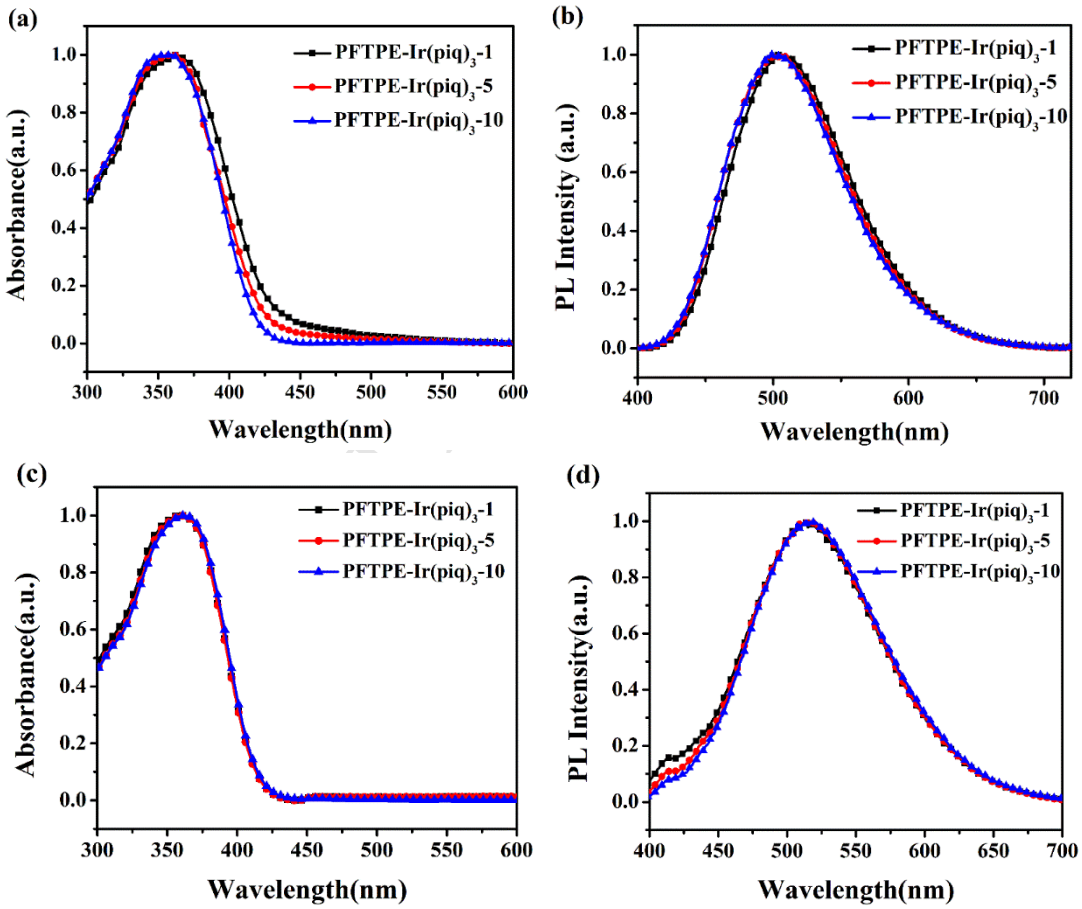

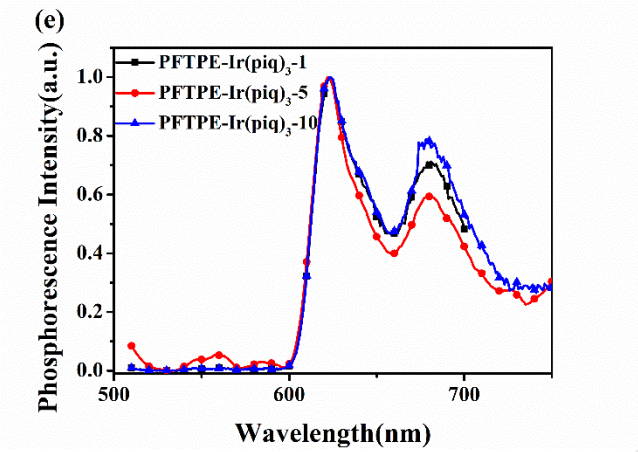


**Fig. 3.** The spectra properties of PFTPE-Ir(piq)$_3$-X: a) the UV-vis absorption spectra in solution; b) the PL spectra in solution; c) the UV-vis absorption spectra in films; d) the PL spectra in films; e) the phosphorescence spectra at 77 K.

As shown in Fig. 3, spectral properties of PFTPE-Ir(piq)$_3$-X were studied as expressed. The UV-vis absorption spectra of PFTPE-Ir(piq)$_3$-X in diluted $CHCl_3$ solution (Fig. 3a) and film (Fig. 3c) all show a strong absorption peak located at about 360 nm which is corresponding to $\pi$–$\pi^*$ transition from the branch chain of PFTPE [3]. The PL spectra of PFTPE-Ir(piq)$_3$-X in diluted $CHCl_3$ solution (Fig. 3b) exhibit emission peak located at around 505 nm attributing to blue-greenish fluorescence of PFTPE. While, in PL spectra of all hyperbranched polymers films (Fig. 3d), the maximum emission peaks of located at around 515 nm, which shows a bathochromic-shift of 10 nm compared with that in diluted $CHCl_3$ solution. It is owing to increasing of conjugation, the molecules are high aggregation states in films [42]. Additional, the emission peaks corresponding to red phosphorescence of Ir(piq)$_3$ in all polymers are not visible, which is identical with our reported work [25, 39]. During PL process of PFTPE-Ir(piq)$_3$-X, it is difficult for Ir(piq)$_3$ to emit red-light excited by FRET from PFTPE to Ir(piq)$_3$ because of low content ratio of Ir(piq)$_3$ unit ($<$1%) in polymers. In Fig. 3e, it can be seen that all polymers of PFTPE-Ir(piq)$_3$-X show shoulder peaks located at 623 nm

corresponding to red phosphorescence of $Ir(piq)_3$ in the phosphorescent spectra of PFTPE-$Ir(piq)_3$-X at 77 K, which could also acquire the triplet energy levels ($E_T$) of 1.99 eV. Moreover, the absolute PL quantum efficiency ($\Phi_{PL}$) of PFTPE-$Ir(piq)_3$-X was measured by integrating sphere. As listed in Table 2, it is interesting to see that all polymers of PFTPE-$Ir(piq)_3$-X exhibit lower $\Phi_{PL}$ in solution and higher $\Phi_{PL}$ in film state, according with typical AIE phenomenon.

**Table 2** The photophysical properties and electrochemical properties of PFTPE-$Ir(piq)_3$-X.

| Polymers | Film (nm) | | Solution (nm) | | $\Phi_{PL}$[c] | $\Phi_{PL}$[a] | HOMO[d] | $E_g$[e] | LUMO[f] |
|---|---|---|---|---|---|---|---|---|---|
| | $\lambda_{abs}$[a] | $\lambda_{PL}$[a] | $\lambda_{abs}$[b] | $\lambda_{PL}$[b] | (%) | (%) | (eV) | (eV) | (eV) |
| PFTPE-$Ir(piq)_3$-1 | 359 | 513 | 363 | 504 | 0.74 | 26.22 | -5.75 | 2.87 | -2.88 |
| PFTPE-$Ir(piq)_3$-5 | 360 | 515 | 360 | 507 | 1.19 | 24.19 | -5.72 | 2.88 | -2.84 |
| PFTPE-$Ir(piq)_3$-10 | 362 | 517 | 359 | 499 | 1.40 | 18.98 | -5.75 | 2.92 | -2.83 |

[a] Measured in neat films.

[b] Measured in $CHCl_3$ solution ($10^{-6}$ mol/L).

[c] Measured in THF. The $\Phi_{PL}$ was measured using an integrating sphere.

[d] Calculated from cyclic voltammetry curve.

[e] Estimated from onset of the absorption spectra ($E_g = 1240/\lambda_{edge}$).

[f] Calculated by the equation $E_{HOMO} = E_{LUMO} - E_g$.

*3.4 Aggregation induced emission enhancement properties*

For exploring the AIE properties of PFTPE-$Ir(piq)_3$-X, their PL behavior in solvent/nonsolvent mixtures were measured as expressed in Fig. 4. During testing, different proportions mixed solutions of water and THF as solvent, the AIE behaviors were inspected

by monitoring the changes in PL spectra with variations in proportion of water in THF. The PL intensity of PFTPE-Ir(piq)$_3$-X is very weak when molecularly dissolved in pure THF, however, it intensifies with increasing water content in THF gradually. And, all polymers of PFTPE-Ir(piq)$_3$-X exhibit higher $\Phi_{PL}$ upon aggregation in the presence of higher percentage of water fraction ($f_w$) in THF-water mixtures than those in pure THF, which is attributing to the introduction of AIEgens of TPE. In pure THF solution, high internal conversion rate results in weak emission owing to intramolecular rotations of phenyl rings of TPE. Nevertheless, in a high percentage of water fraction ($f_w$) in THF-water mixture, these rotations are strongly confined, which restrains nonradiative energy dissipation channels and more efficient emission of PFTPE-Ir(piq)$_3$-X [27-31]. Hence, it can be deduced that polymers of PFTPE-Ir(piq)$_3$-X possess remarkable AIE property.

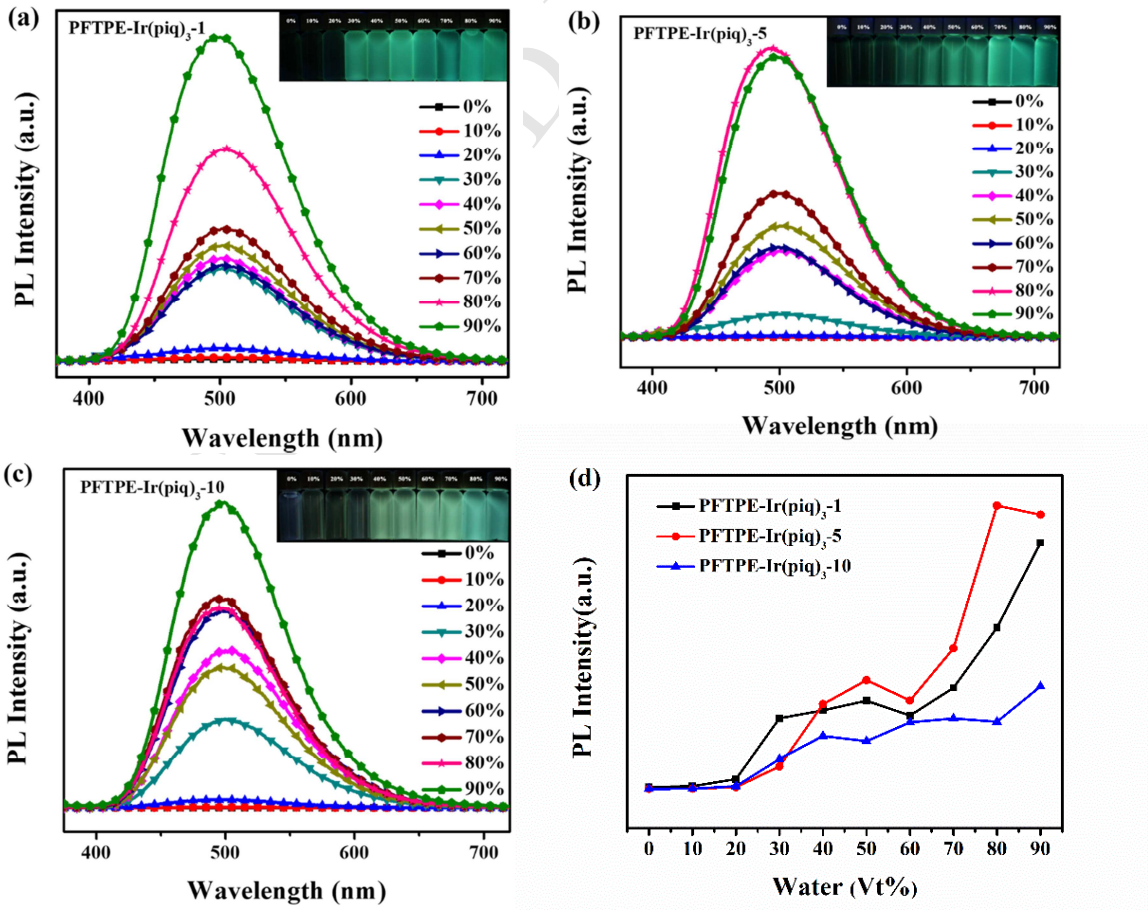

**Fig. 4.** The PL spectra of PFTPE-Ir(piq)$_3$-X in THF-water mixtures with different water fractions (excitation wavelength is 365 nm): a) PFTPE-Ir(piq)$_3$-1; b) PFTPE-Ir(piq)$_3$-5; c) PFTPE-Ir(piq)$_3$-10; d) Variation in PL intensity of PFTPE-Ir(piq)$_3$-X in THF-water mixtures with different water fractions.

**Table 3** The $\Phi_{PL}$ of PFTPE-Ir(piq)$_3$-X in THF-water mixtures with different water fractions.

| Polymers | 0% | 10% | 20% | 30% | 40% | 50% | 60% | 70% | 80% | 90% |
|---|---|---|---|---|---|---|---|---|---|---|
| PFTPE-Ir(piq)$_3$-1 | 0.74 | 1.07 | 2.07 | 10.17 | 14.84 | 16.56 | 10.64 | 13.65 | 21.57 | 44.36 |
| PFTPE-Ir(piq)$_3$-5 | 1.19 | 1.40 | 1.73 | 3.70 | 13.06 | 18.31 | 22.61 | 26.60 | 31.08 | 29.60 |
| PFTPE-Ir(piq)$_3$-10 | 1.40 | 1.21 | 2.15 | 3.88 | 7.37 | 9.51 | 9.89 | 11.05 | 12.52 | 12.74 |

*3.5 Electrochemical properties*

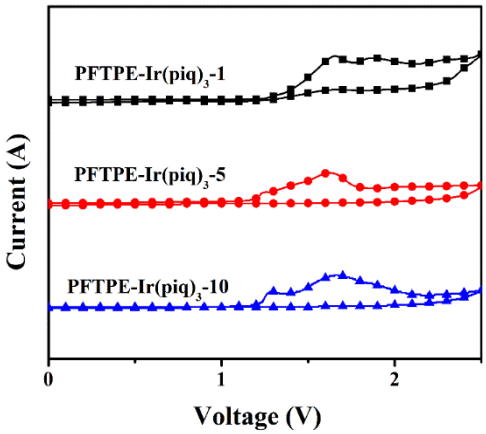


**Fig. 5.** Cyclic voltammetry (CV) curves of PFTPE-Ir(piq)$_3$-X.

As shown in Fig. 5, the electrochemical property of PFTPE-Ir(piq)$_3$-X was measured. The HOMO levels of PFTPE-Ir(piq)$_3$-X were calculated according to the empirical equation $E_{HOMO}$ = - ($E_{ox}$ + 4.4) (eV). The optical band gap was calculated from $E_g$ = 1240/$\lambda_{edge}$, where the $\lambda_{edge}$ is the onset value of the UV-vis absorption spectrum PFTPE-Ir(piq)$_3$-X in solution in the long-wavelength area [25,42]. The LUMO levels of PFTPE-Ir(piq)$_3$-X can be calculated from the HOMO levels and the optical gaps. The HOMO level of PFTPE-Ir(piq)$_3$-5 was -5.72

eV, and the LUMO level was -2.84 eV. The series of PFTPE-Ir(piq)$_3$-X have nearly similar HOMO and LUMO levels owing to low content of Ir(piq)$_3$.

*3.6 Electroluminescent properties*

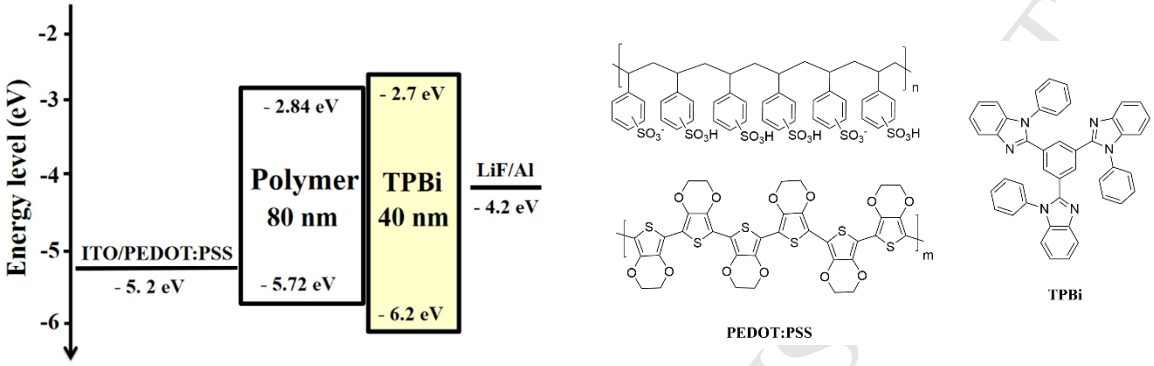


**Fig. 6.** The device structure of WOLED based on PFTPE-Ir(piq)$_3$-X as emission layer.

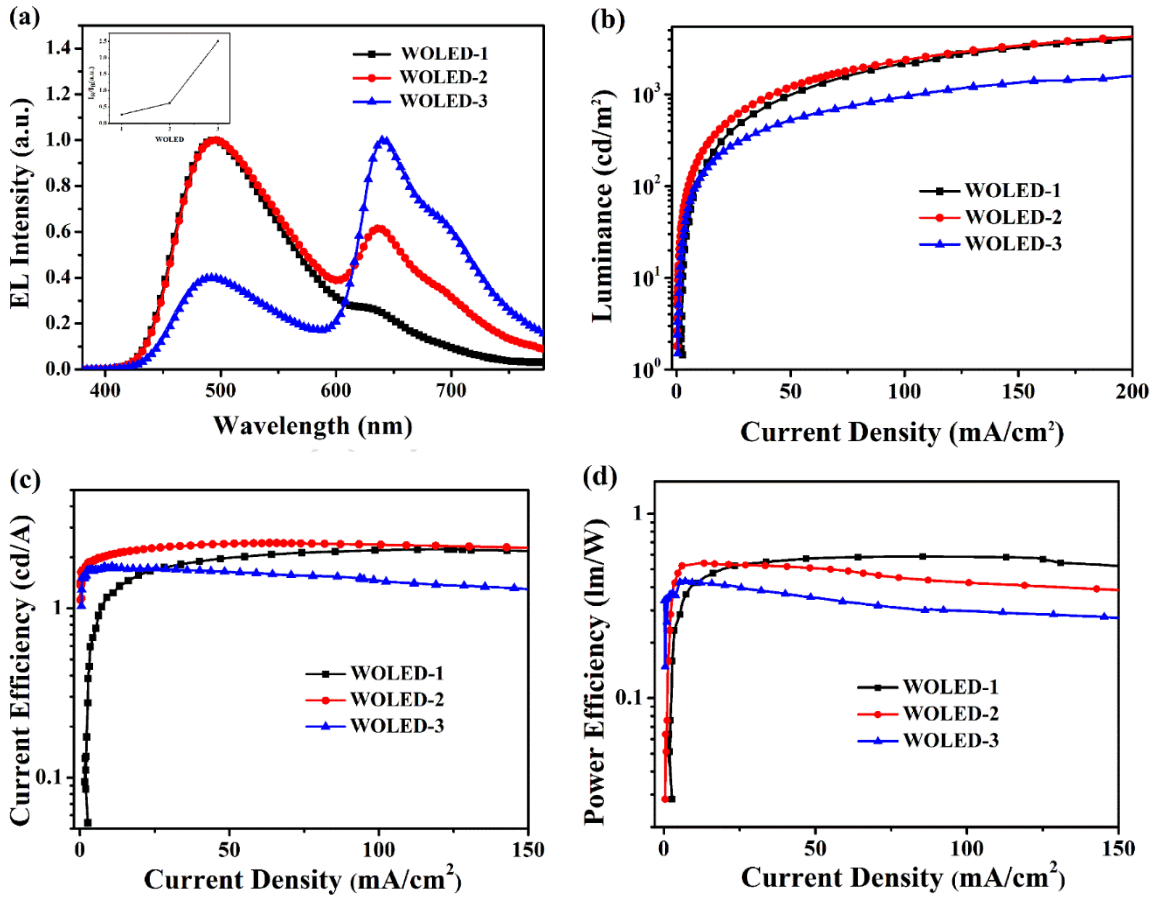

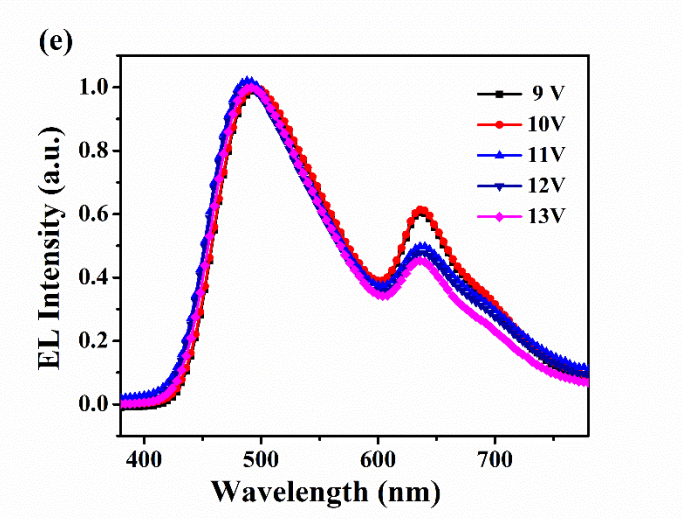


**Fig. 7.** The device performance of WOLED based on PFTPE-Ir(piq)$_3$-X : a) EL spectra ; b) luminance-current density curves; c) current efficiency-current density curves; d) power efficiency- current density curves; e) EL spectra of WOLED-2 at different applied voltages

**Table 4** EL performance of WOLEDs

| Device | Emission layer | $\lambda_{EL}$ (nm) | $Luminance_{max}$ (cd/m$^2$) | $CE_{max}$ (cd/A) | $EQE_{max}$ (%) | CRI | CIE(x, y) |
|---|---|---|---|---|---|---|---|
| WOLED-1 | PFTPE-Ir(piq)$_3$-1 | 492 / 632 | 4067 | 2.24 | 0.91 | 71 | (0.25, 0.36) |
| WOLED-2 | PFTPE-Ir(piq)$_3$-5 | 496 / 636 | 4686 | 2.43 | 1.08 | 86 | (0.26, 0.36) |
| WOLED-3 | PFTPE-Ir(piq)$_3$-10 | 492 / 640 | 2277 | 1.76 | 1.05 | 71 | (0.33, 0.34) |

The favorable AIE properties of PFTPE-Ir(piq)$_3$-X encourage us to investigate their EL performances. As shown in Fig. 7a, the EL spectra of all WOLEDs express blue-greenish emission peaks located at 492 nm originating from PFTPE and red emission peak located at 636 nm originating from Ir(piq)$_3$, which absolutely distinguish with PL spectra of PFTPE-Ir(piq)$_3$-X. In EL spectra, the intensity of red emission peak is much stronger than that in PL spectra. It is since that charge trapping effect of Ir(piq)$_3$ plays dominate role accompanying with FRET from PFTPE to Ir(piq)$_3$ during EL process of PFTPE-Ir(piq)$_3$-X

[7,43]. With increasing content ratio of $Ir(piq)_3$, the red-light emission intensity is enhanced while the blue-greenish light emission intensity is weakened, which induces the intensity ratio of red-light peak to blue-greenish light ($I_R/I_B$) to increase as shown in inset of Fig. 7a. The intensifying in red-light emission with the increase of the content is attributing to stronger charge trapping capability of $Ir(piq)_3$. Accordingly, the corresponding CIE coordinates of WOLED-1, WOLED-2 and WOLED-3 are (0.25, 0.36), (0.26, 0.36) and (0.33, 0.34), respectively. Among them, the WOLED-3 has the best CIE coordinate (0.33, 0.34) close to that of pure white-light (0.33, 0.33), which is superior to the double-color white-light hyperbranched polymer that we reported ever [23]. As expressed in Fig. 7 and Table 4, it can also be seen that the device performance of WOLED-2 are better than those of other two devices and the hyperbranched polymers ever reported [25], which achieves the highest maximum luminance of 4688 cd/m$^2$, the highest maximum current efficiency ($CE_{max}$) of 2.43 cd/A and the highest CRI of 86 among three WOLEDs. More important, as shown in Fig. 7e, the WOLED-2 exhibits excellent device stability. It can be discerned that the EL spectra of WOLED-2 don't nearly vary with raising driven voltage, indicating its better luminous stability.

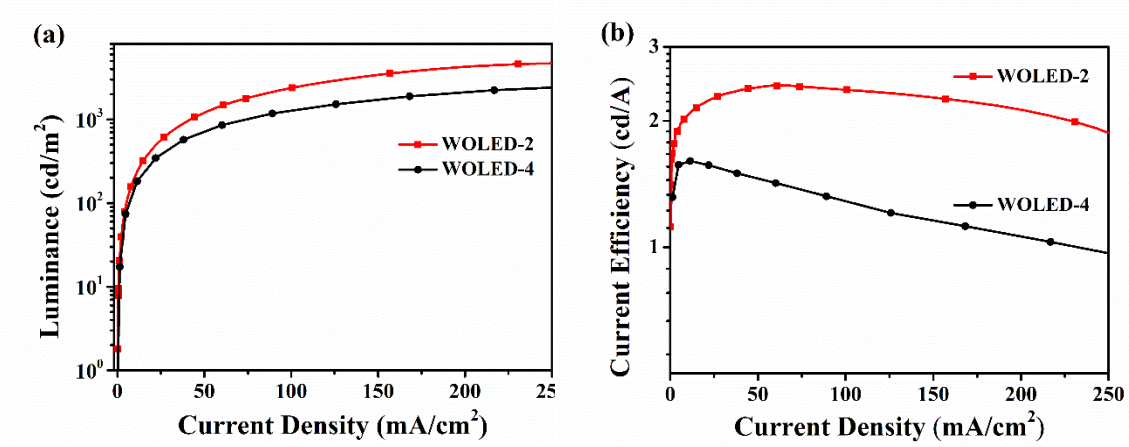

(c)

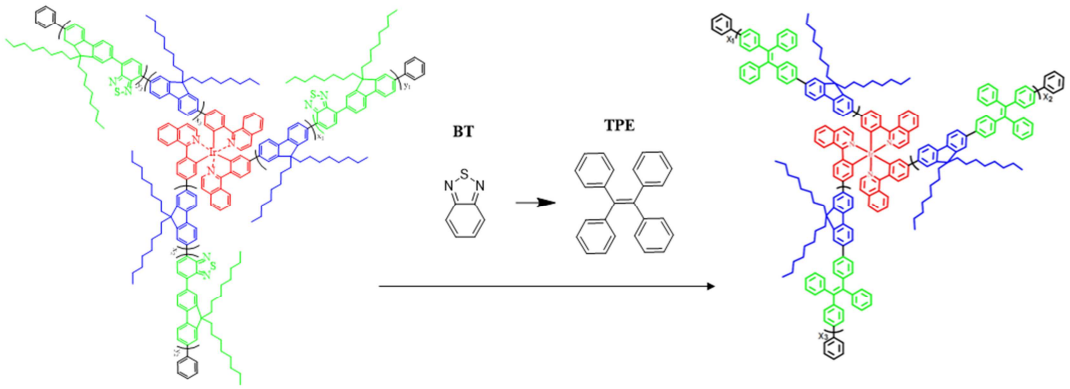


**Fig. 8.** The device performance of WOLED-2 and WOLED-4: a) luminance-current density curves; b) current efficiency-current density curves; c) the chemical molecular structure of hyperbranched polymers of PFBT-Ir(piq)$_3$ and PFTPE-Ir(piq)$_3$.

**Table 5** Percentage decline of current efficiency (CE) with the increase of current density (CD).

| CD (mA/cm$^2$) | WOLED-2 | | WOLED-4 | |
|---|---|---|---|---|
| | CE (cd/A) | Decline (%) | CE (cd/A) | Decline (%) |
| 50 | 2.41 | 0.8 | 1.46 | 8.7 |
| 100 | 2.37 | 2.4 | 1.25 | 21.9 |
| 150 | 2.26 | 6.9 | 1.15 | 28.1 |
| 200 | 2.12 | 12.7 | 1.05 | 34.4 |

For explanation of perfect function of AIEgen on white-light hyperbranched polymers, we also fabricated WOLED-4 with device structure of ITO / PEDOT:PSS (40 nm) / PFBT-Ir(piq)$_3$ (80 nm) / TPBi (40 nm) / LiF (1 nm) / Al (100 nm) (Fig. 6), in which the white-light hyperbranched polymer of PFBT-Ir(piq)$_3$ reported by our early works acted as emission layer [25]. In PFBT-Ir(piq)$_3$, the green-light unit of 2,1,3-benzothiadiazole (BT) exhibits no AIE effect, which is different from TPE. As expressed in Fig. 8a, it can be seen that the device WOLED-2 achieves the maximum luminance of 4688 cd/m$^2$, which is higher than that of WOLED-4 (3267 cd/m$^2$). By comparing with current efficiency-current density curves of WOLED-2 and WOLED-4 (as expressed in Fig. 8b and Table 5), it can be found

that the WOLED-4 exhibited more remarkable efficiency roll-off with increasing current density relative to that of WOLED-2. For example, the current efficiency of WOLED-2 only dropped 12.7% with current density increasing from 50 mA/cm$^2$ to 200 mA/cm$^2$, however, the current efficiency of WOLED-4 dropped 34.4% with current density increasing from 50 mA/cm$^2$ to 200 mA/cm$^2$. It is since that introduction of AIEgens of TPE in branches chains is expected to restrain ACQ conjugation chains and improve efficiency stability of white-light hyperbranched polymer eventually. Meanwhile, Ir(piq)$_3$ is encircled by PFTPE branches chains in hyperbranched structure, which effectively suppresses concentration quenching and triplet-triplet (T-T) annihilation [3,25]. Therefore, the efficiency roll-off could be restrained effectively.

## 4. Conclusion

In summary, the new-style white-light hyperbranched polymers with PFTPE as branches and Ir(piq)$_3$ as cores exhibit AIE characteristic. By tuning the contents ratio of Ir(piq)$_3$, the optimized white-light hyperbranched polymers are acquired and the EL spectra can cover the entire visible area from 400 nm to 780 nm. When the content ratio of Ir(piq)$_3$ is 0.5 mol%, the WOLED-2 based on PFTPE-Ir(piq)$_3$-5 exhibits a high CRI of 86, with maximum luminance of 4686 cd/m$^2$, maximum current efficiency of 2.43 cd/A and a maximum external quantum efficiency of 1.08%. Furthermore, it exhibits lower efficiency roll-off phenomenon, which is owing to introduction of AIEgen of TPE in white-light hyperbranched polymer.

## Acknowledgements

This work was financially supported by Program for National Natural Scientific Foundation of China (61775155, 61705158, 61605138); Shanxi Provincial Key Innovative

Research Team in Science and Technology (201605D131045-10); Natural Science Foundation of Shanxi Province (201601D011031, 201601D202030); Open Foundation of State Key Laboratory of Electronic Thin Films and Integrated Devices (KFJJ201507); Basic and Frontier Research Program of Chongqing Municipality (cstc2015jcyjA50036); Natural Science Foundation of Yongchuan District (Ycstc, 2015nc4001).

**References**

[1] J. Kido, K. Hongawa, K. Okuyama, K. Nagai, Appl. Phys. Lett. 64 (1994) 815-817.

[2] H. Sasabe, J. Kido, J. Mater. Chem. C. 1 (2013) 1699-1707.

[3] J. Sun, H. Wang, H. Xu, T. Zhang, L. Li, J. Li, Dyes Pigm. 130 (2016) 191-201.

[4] D. Zhao, W. Huang, H. Guo, H. Wang, J.S. Yu, Mater. Sci. Eng B. 218 (2017) 7-13.

[5] B.Q. Liu, H. Nie, X.B. Zhou, S.B. Hu, D.X. Luo, D.Y. Gao, J.H. Zou, M. Xu, L. W, Z.J. Zhao, A.J. Qin, J.B. Peng, H.L. Ning, Y. Cao, B.Z. Tang, Adv. Funct. Mater. 26 (2016) 776–783.

[6] G. Cheng, T. Fei, Y. Zhao, Y.G. Ma, S.Y. Liu, Org. Electron. 11 (2010) 498-502.

[7] J.S. Wang, X.J. Xu, Y. Tian, C. Yao, L.D. Li, Synth. Met. 197 (2014) 90-98.

[8] C. Fan, Y.H. Li, C.L. Yang, H.B. Wu, J.G. Qin, Y. Cao, Chem. Mater. 24 (2012) 4581-4587.

[9] M. Zhu, J. Zou, S. Hu, C. Li, C. Yang, H. Wu, J. Phys. Chem. 22 (2012) 361-366.

[10] H. Wu, G. Zhou, J. Zou, C.L. Ho, W.Y. Wong, W. Yang, Adv. Mater. 21 (2009) 4181-4184.

[11] J. Zou, H. Wu, C.S. Lam, C. Wang, J. Zhu, C. Zhong, Adv. Mater. 23 (2011) 2976-2980.

[12] Y. Zhou, Q. Sun, Z. Tan, H. Zhong, C. Yang, Y. Li, J. Phys. Chem. C. 111 (2007)

6862-6867.

[13] E. Williams, K. Haavisto, J. Li, G. Jabbour, Adv. Mater. 19 (2007) 197-202.

[14] P. Shih, Y. Tseng, F. Wu, K. Dixit, C. Shu, Adv. Funct. Mater. 16 (2006) 1582-1589.

[15] B. Zhang, C. Qin, J. Ding, L. Chen, L. Xie, Y. Cheng, Adv. Funct. Mater. 20 (2010) 2951-2957.

[16] G. Tu, C. Mei, Q. Zhou, Y. Cheng, Y. Geng, L. Wang, Adv. Funct. Mater. 16 (2006) 101-106.

[17] J. Liu, Q. Zhou, Y. Cheng, Y. Geng, L. Wang, D. Ma, Adv. Funct. Mater. 16 (2007) 957–965.

[18] J. Liu, Y. Cheng, Z. Xie, Y. Geng, L. Wang, X. Jing, Adv. Mater. 20 (2008) 1357-1362.

[19] J. Liu, Q. Zhou, Y. Cheng, Y. Geng, L. Wang, D. Ma, Adv. Mater. 17 (2010) 2974-2978.

[20] L. Chen, P.C. Li, H. Tong, Z.Y. Xie, L.X. Wang, X.B. Jing, J. Polym. Sci. Part A Polym. Chem. 50 (2012) 2854-2862.

[21] M.R. Zhu, Y.H. Li, X.S. Cao, B. Jiang, H.B. Wu, J.G. Qin, Macromol. Rapid Commun. 35 (2014) 2071-2076.

[22] K. Zhang, Z. Chen, C.L. Yang, S.L. Gong, J.G. Qin, Y. Cao, Macromol. Rapid Commun. 27 (2006) 1926-1931.

[23] J. Sun, J. Yang, C. Zhang, H. Wang, J. Li, S. Su, New J. Chem. 39 (2015) 5180-5188.

[24] J. Sun, D.Y. Wu, L. Gao, M.N. Hou, G.J. Lu, J. Li, X.W. Zhang, Y.Q. Miao, H. Wang, B.S. Xu, RSC Adv. 8 (2018) 1638–1646.

[25] J. Sun, H. Wang, T. Yang, X. Zhang, J. Li, T. Zhang, Dyes Pigm. 125 (2016) 339-347.

[26] J. Luo, Z. Xie, J. Lam, L. Cheng, H. Chen, C. Qiu, Chem. Commun. 18 (2001)

1740-1741.

[27] L. Xing, X. Wang, J. Zhang, Z. Zhou, S. Zhuo, Polym. Chem. 7 (2015) 515-518.

[28] Z. Zhao, S. Chen, X. Shen, F. Mahtab, Y. Yu, P. Lu, Chem. Commun. 46 (2010) 686–688.

[29] Z. Zhao, Z. Chang, B. He, B. Chen, C. Deng, P. Lu, Chemistry. 19 (2013) 11512-11517.

[30] Z. Liu, W. Xue, Z. Cai, F. Mahtab, Y. Yu, P. Lu, J. Mater. Chem. 21 (2011) 14487-14491.

[31] A. Islam, D.D. Zhang, R.X. Peng, R.J. Yang, L. Hong, W. Song, Q. Wei, L. Duan, Z.Y. Ge, Chem. Asian J. 12 (2017) 2189-2196.

[32] A. Islam, D.D. Zhang, X.H. Ouyang, R.J. Yang, T. Lei, L. Hong, R.X. Peng, L.Duan, Z.Y. Ge, J. Mater. Chem. C. 5 (2017) 6527-6536.

[33] E. Ravindran, E. Varathan, V. Subramanian, V. Subramanian, N. Somanathan, J. Mater. Chem. C. 3 (2015) 4359-4371.

[34] T. Guo, R. Guan, J.H. Zou, J. Liu, L. Ying, W. Yang, Polym. Chem. 2 (2011) 2193-2203.

[35] T. Guo, L. Yu, B.F. Zhao, Y.H. Li, Y. Tao, W. Yang, Macromol. Chem. Phys. 213 (2012) 820-828.

[36] J. Liu, L. Yu, C.M. Zhong, R.F. He, W. Yang, H.B. Wu, RSC Adv. 2 (2011) 689-696.

[37] P. Lu, J.W.Y. Lam, J. Liu, C.K.W. Jim, W. Yuan, C.Y.K. Chan, N. Xie, Q. Hu, K.K.L. Cheuk, B.Z. Tang, Macromolecules. 44 (2011) 5977-5986.

[38] C.L .Tao, B. Chen, X.G. Liu, L.J. Zhou, X.L. Zhu, J. Cao, Z.G. Gu, Z.J. Zhao, L. Shen, B.Z. Tang, Chem. Commun. 53 (2017) 9975—9978.

[39] H. Wang, Y. Xu, T.J. Tsuboi, H.X. Xu, Y.L. Wu, Z.X. Zhang, Y.Q. Miao, Y.Y. Hao, X.G. Liu, B.S. Xu, W. Huang, Org. Electron. 14 (2013) 827–838.

[40] L. Ying, J.H. Zou, W. Yang, A.Q. Zhang, Z.L. Wu, W. Zhao, Dyes Pigm. 82 (2009)

251-257.

[41] Q.L. Chen, N.L. Liu, L. Ying, W. Yang, H.B. Wu, W. Xu, Polymer. 50 (2009) 1430-1437.

[42] T.M. Zhang, J. Sun, X.Q. Liao, M.N. Hou, W.H. Chen, J. Li, H. Wang, L. Li, Dyes Pigm. 139 (2017) 611-618.

[43] P. Tao, Y.B. Zhang, J. Wang, L.W. Wei, H.X. Li, X.L. Li, Q. Zhao, X.W. Zhang, S.J. Liu, H. Wang, W. Huang, J. Mater. Chem. C. 5 (2017) 9306-9314.

## Highlights

1. Hyperbranched white polymers with aggregation-induced emission property were synthesized
2. The new-style hyperbranched white polymers with PFTPE as branches and $Ir(piq)_3$ as cores are conducive to achieve the full-band emission
3. The WOLEDs using PFTPE-$Ir(piq)_3$-X as emission layer show nearly no efficiency roll-off under high current density